Cell Reports
Article

Mpn1, Mutated in Poikiloderma with Neutropenia Protein 1, Is a Conserved 3′-to-5′ RNA Exonuclease Processing U6 Small Nuclear RNA

Vadim Shchepachev,[1] Harry Wischnewski,[1] Edoardo Missiaglia,[2] Charlotte Soneson,[2] and Claus M. Azzalin[1,*]
[1]Institute of Biochemistry (IBC), Eidgenössische Technische Hochschule Zürich (ETHZ), Zürich, CH-8093, Switzerland
[2]Bioinformatics Core Facility, SIB Swiss Institute of Bioinformatics, Lausanne, CH-1015, Switzerland
*Correspondence: claus.azzalin@bc.biol.ethz.ch
http://dx.doi.org/10.1016/j.celrep.2012.08.031

SUMMARY

Clericuzio-type poikiloderma with neutropenia (PN) is a rare genodermatosis associated with mutations in the C16orf57 gene, which codes for the uncharacterized protein hMpn1. We show here that, in both fission yeasts and humans, Mpn1 processes the spliceosomal U6 small nuclear RNA (snRNA) posttranscriptionally. In Mpn1-deficient cells, U6 molecules carry 3′ end polyuridine tails that are longer than those in normal cells and lack a terminal 2′,3′ cyclic phosphate group. In *mpn1*Δ yeast cells, U6 snRNA and U4/U6 di-small nuclear RNA protein complex levels are diminished, leading to precursor messenger RNA splicing defects, which are reverted by expression of either yeast or human Mpn1 and by overexpression of U6. Recombinant hMpn1 is a 3′-to-5′ RNA exonuclease that removes uridines from U6 3′ ends, generating terminal 2′,3′ cyclic phosphates in vitro. Finally, U6 degradation rates increase in *mpn1*Δ yeasts and in lymphoblasts established from individuals affected by PN. Our data indicate that Mpn1 promotes U6 stability through 3′ end posttranscriptional processing and implicate altered U6 metabolism as a potential mechanism for PN pathogenesis.

INTRODUCTION

Clericuzio-type poikiloderma with neutropenia (PN) is an autosomal-recessive hereditary disorder characterized by a papular erythematous rash that starts on the limbs and face during the first year of life and evolves into diffuse poikiloderma and pachyonychia, especially of the toenails. PN also features chronic neutropenia and bone marrow abnormalities, leading to infections mainly of the respiratory system and eventually to myelodysplasia associated with the risk of leukemic transformation (Arnold et al., 2010; Chantorn and Shwayder, 2012; Clericuzio et al., 2011; Clericuzio et al., 1991; Colombo et al., 2012; Concolino et al., 2010; Piard et al., 2012; Tanaka et al., 2010; Volpi et al., 2010; Walne et al., 2010). To date, 38 PN patients have been reported in the literature, and they bear 19 different mutations in the gene C16orf57 (Arnold et al., 2010; Chantorn and Shwayder, 2012; Clericuzio et al., 2011; Colombo et al., 2012; Concolino et al., 2010; Piard et al., 2012; Tanaka et al., 2010; Volpi et al., 2010; Walne et al., 2010), which encodes a 247 amino acid protein herein referred to as hMpn1 (for *m*utated in *PN* protein *1*). Several PN patients have been misdiagnosed with dyskeratosis congenita (DC) or Rothmund-Thomson syndrome (RTS) because of a large overlap of the clinical manifestations of these syndromes (Colombo et al., 2012; Walne et al., 2010). Therefore, the screening of DC and RTS patients of thus-far-unknown genetic origin for mutations in the C16orf57 gene is expected to rapidly augment the number of known PN patients in the near future. Although structure prediction algorithms have assigned hMpn1 to the superfamily of 2H phosphodiesterases found in bacteria, archaea, and eukaryotes (Colombo et al., 2012; Mazumder et al., 2002), its functions remain completely obscure. This superfamily comprises at least four families of RNA-modifying enzymes, including bacterial 2′–5′ RNA ligases, fungal RNA ligases, plant and yeast 1′,2′ cyclic nucleotide phosphodiesterases, and mammalian 2′,3′ cyclic nucleotide phosphodiesterases. Two catalytically active tetrapeptide motifs (H-X-T/S-X, where X is a hydrophobic residue) are found in all 2H phosphodiesterase superfamily members, and they correspond to $H_{120}L/S_{122}L$ and $H_{208}L/S_{210}L$ sequences in hMpn1 (Colombo et al., 2012; Mazumder et al., 2002).

In eukaryotes, introns within a precursor messenger RNA (pre-mRNA) transcript are removed by the spliceosome (for reviews, see: Valadkhan, 2010; Wahl et al., 2009; Will and Lührmann, 2011). A core component of the active spliceosome is the small nuclear RNA (snRNA) U6, an evolutionarily conserved noncoding RNA (ncRNA) of approximately 100 bases produced by RNA polymerase III (RNAPIII). U6 participates in the formation of the active site of the spliceosome and catalyzes the transesterification reactions that occur during splicing. At the onset of spliceosome assembly, U6 and U4, another spliceosomal snRNA, associate into a di-snRNA protein complex (U4/U6 di-snRNP) wherein the two transcripts are base paired in a catalytically inactive state. Unwinding of the U4-U6 duplex by the conserved Brr2p/SNRNP200 helicase and release of U4 convert the spliceosome into a catalytically active form (for reviews, see: Valadkhan, 2010; Wahl et al., 2009; Will and Lührmann, 2011). U6 and U4 molecules previously engaged in a splicing

cycle can be recycled and reassembled into new U4/U6 di-snRNPs for participation in a new round of splicing. Failure to recycle U6 leads to impaired U4/U6 di-snRNP assembly and accumulation of free U4 snRNA in yeast, and this defect can be rescued by overexpression of U6 snRNA (Chen et al., 2006). Several factors have been shown to assist U6 recycling, including members of the evolutionarily conserved nineteen complex (NTC) and the Sm-like 2–8 (LSm2–8) ring complex (Achsel et al., 1999; Lygerou et al., 1999).

Newly transcribed U6 contains four template 3′ end uridine (U) residues that are immediately bound by the La antigen (Kunkel et al., 1986; Rinke and Steitz, 1985; Stefano, 1984), whereas in mature U4/U6 di-snRNPs, the La antigen is superseded by the LSm2–8 complex (Achsel et al., 1999; Mayes et al., 1999; Salgado-Garrido et al., 1999; Séraphin, 1995; Vidal et al., 1999). The La-to-LSm exchange is a prerequisite for U4/U6 di-snRNP formation, given that the LSm2–8 complex recruits the Prp24/p110 RNA-binding protein, which promotes the annealing of U4 and U6 (Bell et al., 2002; Martin-Tumasz et al., 2011; Pannone et al., 1998; Raghunathan and Guthrie, 1998; Ryan et al., 2002). U6 snRNA molecules are remarkably heterogeneous due to extensive posttranscriptional modification of their 3′ termini. Whereas the large majority of cellular U6 molecules contain a short 3′ oligo(U) tail comprising five Us blocked by a cyclic 2′,3′ phosphate 3′ end group (>p group), a small fraction of U6 (~10%) can contain 3′ oligo(U) stretches up to 20 nucleotides long terminating with a *cis*-2′,3′-diol end group (-OH) (Lund and Dahlberg, 1992; Rinke and Steitz, 1985; Terns et al., 1992). The dynamic balance between these two major forms of U6 is determined by two counteracting enzymatic activities that elongate and trim U6 oligo(U) tails (Gu et al., 1997; Tazi et al., 1993; Trippe et al., 2003). The enzyme uridylylating U6 3′ end has been identified in humans, and it corresponds to the terminal uridylyltransferase (TUTase) (Trippe et al., 2006). In contrast, the nuclease that trims the 3′ terminus of U6 has not yet been isolated, and the functional significance of these structural variants of U6 remains obscure. Here, we reveal that Mpn1 proteins are evolutionarily conserved 3′-to-5′ RNA exonucleases that specifically trim U6 oligo(U) and generate U6 molecules terminating with >p groups. Mpn1-mediated processing of U6 transcripts prevents their degradation. Our data unveil an unanticipated cellular pathway dictating the fate of U6 molecules and implicate altered U6 processing as a potential mechanism for PN pathogenesis.

RESULTS

Deletion of *mpn1*$^+$ Leads to a Generalized Pre-mRNA Splicing Defect and to Diminished U6 Cellular Levels in Fission Yeast

While screening a complete gene deletion collection of *Schizosaccharomyces pombe* strains for regulators of telomere transcription, we isolated the putative ortholog of hMpn1 (*SPAC23C11.10*, herein referred to as *mpn1*$^+$; the screening will be presented elsewhere). *mpn1*Δ cells displayed higher amounts of telomeric repeat-containing RNA (TERRA) (Azzalin et al., 2007; Bah et al., 2012) and shorter telomeres compared to wild-type (WT) strains (Figures S1A and S1B). In addition, *mpn1*Δ cells showed a mild slow-growth phenotype at the standard temperature of 30°C. This phenotype was exacerbated in the cold (20°C), whereas *mpn1*Δ cells grew at rates similar to WT at 36°C (Figure 1A). Northern blot and RT-PCR analyses revealed that *mpn1*$^+$-deleted strains suffered a generalized pre-mRNA splicing defect, as shown by the accumulation of pre-mRNA transcripts comprising introns of different lengths (*TBP1*, *SPBC660.16*, and *DBP2*; Figures S1C and S1D). The spliceosome-dependent processing of the telomerase RNA component Ter1 (Box et al., 2008) was also impaired, and premature, catalytically inactive Ter1 accumulated in *mpn1*Δ cells (Figure S1D). It is possible that the lack of complete Ter1 processing and the possible missplicing of pre-mRNAs coding for other telomeric factors account for the aberrant telomere length and TERRA accumulation observed in the deleted strains (Figures S1A and S1B). Moreover, telomere-length abnormalities appear not to be an evolutionarily conserved feature of Mpn1 deficiency, given that cells established from PN patients carry telomeres of normal length (Walne et al., 2010). Nevertheless, we do not exclude the possibility that *mpn1*$^+$ deletion might also affect telomere-length homeostasis and TERRA cellular levels by processing RNA molecules directly involved in telomere maintenance.

We also tested for splicing of the U6 snRNA, which in fission yeast comprises an intron of approximately 50 bases posttranscriptionally removed by the spliceosome (Tani and Ohshima, 1989). As for the other substrates, unspliced U6 accumulated in *mpn1*Δ cells, and mature, spliced U6 was approximately 40% less abundant (Figures 1B, 2A, S1C and S1D). Total (spliced plus unspliced) U6 transcripts in *mpn1*Δ cells were approximately 30% fewer than in WT cells, as judged by real-time quantitative RT-PCR (Figure 3A). On the contrary, *mpn1*$^+$ deletion did not substantially affect the total levels of 5S ribosomal RNA (rRNA) and U5 spliceosomal snRNA (Figure 1B). Interestingly, the splicing defects observed in *mpn1*$^+$-deleted cells were enhanced in the cold and partly resolved at 36°C, at least in terms of accumulation of spliced RNA species, as shown by northern blot analysis, wherein 18S rRNA signals were used for normalizing the ones from spliced mRNAs (Figure S1E). This suggests that the growth defects associated with *mpn1*$^+$ deletion could be derived from improper pre-mRNA splicing.

Deletion of *mpn1*$^+$ Leads to Improper Processing of the U6 3′ End Oligo(U) Tail and Diminished Levels of U4/U6 di-snRNPs

High-resolution denaturing PAGE followed by northern blotting with the use of U6 probes showed that mature U6 ran slower in *mpn1*Δ cells (Figure 1B). We performed 3′ rapid amplification of complementary DNA (cDNA) ends (3′ RACE) and found that most U6 oligo(U) tracts contained five Us in WT and six Us in *mpn1*Δ cells (Figure 1C). Moreover, in WT cells, the large majority of U6 snRNA terminated with a 3′ end U containing a >p group; in fact, treatment with polynucleotide kinase (PNK) in mild acidic conditions (a treatment known to release terminal >p groups from RNA molecules), but not with calf intestinal phosphatase (CIP, which is unable to release >p groups), converted mature U6 into a more slowly migrating form (Figure 1B) and rendered it accessible to poly(A) polymerase (PAP)-mediated nucleotide

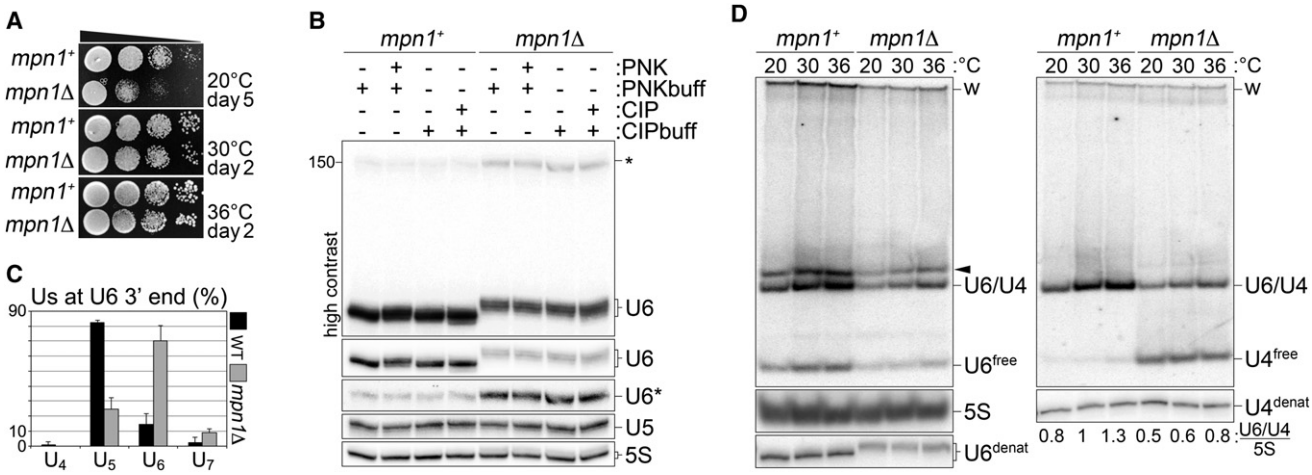

Figure 1. Cellular Consequences of *mpn1*$^{+}$ Deletion

(A) Replicates of serial dilutions of the indicated yeasts were spotted on complete medium and grown at 20°C, 30°C, or 36°C. Images were taken after 2 or 5 days of incubation.

(B) Total RNA was treated with T4 PNK in mild acidic conditions, CIP, or reaction buffer (buff) and separated in denaturing polyacrylamide gels. Mature U6, intron-containing U6 (asterisk), U5 snRNA, and 5S rRNA were visualized via northern blotting. The position of a size marker of 150 bases is shown on the left.

(C) 3′ RACE analysis of U6 oligo(U) tails. Bars and error bars are averages of the number of Us within U6 olgo(U) tails and SEM from three independent experiments.

(D) Yeasts were grown at 20°C, 30°C, or 36°C, and RNA was extracted and separated in nondenaturing conditions. The same membrane was hybridized successively with U6, U4, and 5S oligonucleotides. U6/U4 di-snRNPs and free U6 and U4 are indicated. The arrowhead points to a slowly migrating U6 complex of unknown origin that is devoid of U4 molecules. Wells are indicated with "w". "U6^{denat}" and "U4^{denat}" indicate U6 and U4 detected in denaturing polyacrylamide gels with the use of the same RNA prepared for di-snRNP analysis. Numbers on the right indicate the ratio between the U6/U4 di-snRNP signal and the 5S signal, after normalization through the signal corresponding to *mpn1*$^{+}$ cells grown at 30°C.

See also Figures S1, S2, and S3.

addition (Figure S2A). In contrast, in *mpn1*Δ cells, PNK treatment did not affect the U6 run, nor was it needed to allow PAP-mediated extension of U6 (Figures 1B and S2A). The electrophoretic mobility of 5S rRNA and U5 snRNA remained unchanged in all tested conditions (Figure 1B). We conclude that, in *mpn1*$^{+}$-deleted cells, the U6 oligo(U) tails are longer than in normal cells and terminate with an -OH group. The molecular defects that accrue on U6 in *mpn1*Δ cells are not a secondary consequence

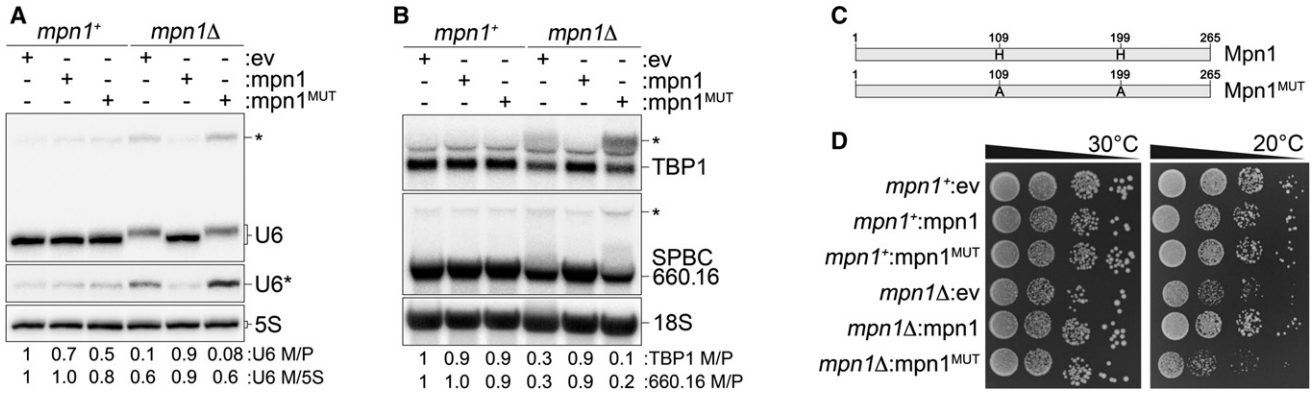

Figure 2. Mpn1 Rescues the Cellular Defects of *mpn1*Δ Cells

(A) Northern blot analysis of U6 in the indicated yeast cells stably transformed with WT Mpn1 or Mpn1^{MUT} expression vectors or with control ev. Numbers indicate ratios between the signal associated with mature (M) and premature (P; unspliced) U6 after normalization through the U6 signal associated with *mpn1*$^{+}$ cells carrying ev.

(B) Splicing of the indicated transcripts was analyzed via northern blotting. Asterisks indicate pre-mRNAs. Numbers indicate ratios between the signal associated to mature and premature transcripts after normalization through *mpn1*$^{+}$ ev samples.

(C) Schematic representation of yeast Mpn1 proteins. Mpn1^{MUT} carries histidine to alanine substitutions at the indicated positions.

(D) Replicates of serial dilutions of the indicated yeasts were spotted on complete medium and grown at 20°C or 30°C.

See also Figures S2 and S4.

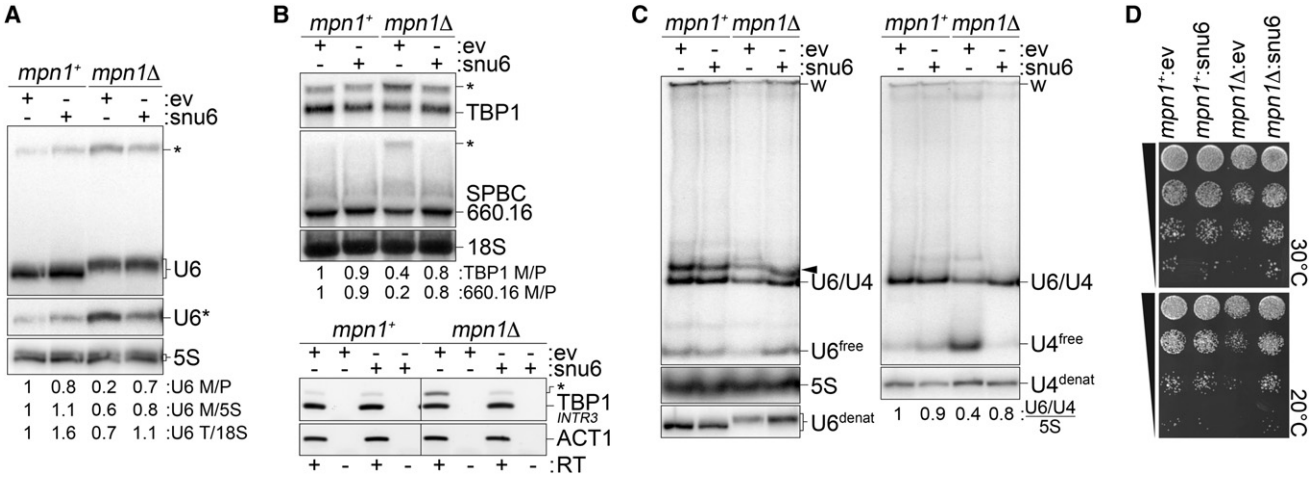

Figure 3. Enhanced U6 Expression Rescues the Cellular Defects of *mpn1*Δ Cells

(A) Northern blot analysis of U6 in strains stably transformed with plasmids carrying one copy of U6 gene (*snu6*$^+$) or with ev. Numbers at the bottom are normalized ratios between mature and premature U6 signals (M/P), mature U6 and 5S signals (M/5S), and total (T) U6 and 18S rRNA, as measured by quantitative real-time RT-PCR.

(B) Splicing of the indicated transcripts was analyzed via northern blotting (upper panels) and RT-PCR (lower panels). Asterisks indicate pre-mRNAs. Numbers below northern blots (upper panels) are as in Figure 2B. For TBP1 RT-PCR, primer pairs spanning the third intron (*INTR3*) were used. Intronless *act1*$^+$ mRNA was amplified to control for loading. RT, reverse transcription.

(C) Analysis of U4/U6 di-snRNP levels in the indicated strains. Numbers and labeling are as in Figure 1D.

(D) Replicates of serial dilutions of the indicated yeasts were spotted on complete medium and grown at 20°C or 30°C.

See also Figure S2.

of impaired pre-mRNA splicing, because strains in which the unrelated splicing factor Prp1 (Potashkin et al., 1989) was inhibited showed severely compromised global splicing (Figure S3A), and yet U6 RNA, although present at low levels, ran normally in polyacrylamide gels (Figure S3B). Analysis of U4/U6 di-snRNPs in native polyacrylamide gels revealed that free U4 accumulated in *mpn1*Δ cells at standard temperatures, whereas the levels of U4/U6 di-snRNPs diminished to extents similar to the ones measured for mature U6 snRNA (Figures 1D and 2A). The levels of di-snRNPs were further diminished at 20°C and were augmented at 36°C (Figure 1D). These data strongly indicate that in absence of Mpn1, lower levels of U6 are available for di-snRNP complex assembly, thereby leading to the accumulation of free U4, lower U4/U6 di-snRNP levels, and, most likely, inefficient pre-mRNA splicing.

The Integrity of the Tetrapeptide Motifs of Mpn1 Is Essential for Its Function In Vivo

We generated *mpn1*$^+$ and *mpn1*Δ strains overexpressing C-terminally myc-tagged, WT Mpn1. Ectopic Mpn1 expression in *mpn1*Δ cells rescued U6 aberrations, pre-mRNA splicing defects, and slow growth in the cold, but did not affect any of these characteristics in WT cells (Figures 2A–2D). Thus, the above-described phenotypes are true outcomes of *mpn1*$^+$ deletion. We also generated strains expressing a myc-tagged variant of Mpn1 (Mpn1^{MUT}) wherein the two putative catalytic histidines within its tetrapeptide motifs (H109 and H199) are mutagenized into alanines (Figure 2C). Mpn1^{MUT} was unable to restore normal U6 processing and further impaired pre-mRNA splicing and cell growth in the cold when overexpressed in *mpn1*Δ cells (Figures 2A–2D), indicating that H109 and H199 are essential for Mpn1 function in vivo. Mpn1 and Mpn1^{MUT} were expressed at comparable levels in WT and *mpn1*Δ cells (Figure S4A), excluding the possibility that the inability of Mpn1^{MUT} to rescue the phenotypes associated with the deletion of *mpn1*$^+$ was due to insufficient protein expression. Both ectopically expressed Mpn1 variants coimmunoprecipitated with U6 RNA, but not with 5S rRNA, in immunoprecipitation (IP) experiments with myc antibodies (Figure S4A). This suggests that Mpn1 interacts, directly or indirectly, with U6 in vivo independently of H109 and H199. The ability of Mpn1 to interact with U6 is further supported by the observation that myc-tagged Mpn1 expressed from its endogenous promoter localizes mainly to the nucleus (Figure S4F).

The Pre-mRNA Splicing Defects in *mpn1*Δ Cells Are Compensated by Overexpression of U6

In order to restore normal U6 levels in *mpn1*Δ cells, we generated strains carrying one additional copy of the U6 gene (*snu6*$^+$) stably integrated at the *aur1*$^+$ locus. Compared to WT strains carrying empty vector plasmids (ev), the levels of total U6 (spliced plus unspliced) increased 1.6-fold and 1.1-fold in *mpn1*$^+$ and *mpn1*Δ cells, respectively, with extra snu6 (Figure 3A). U6 molecules remained longer in *mpn1*Δ:snu6 cells than in WT cells and were devoid of terminal >p groups, whereas the defects in splicing and in U4/U6 di-snRNP cellular levels were essentially resolved (Figures 3A–3C and S2B). Expression of an intronless U6 gene stably integrated at the *aur1*$^+$ locus also restored the splicing defects in *mpn1*Δ, whereas it did not affect splicing in WT strains (data not shown). Importantly, the slow-growth phenotype induced by cold temperature was also rescued by *snu6*$^+$ expression (Figure 3D). Therefore, additional newly transcribed U6 can compensate for the splicing defects associated

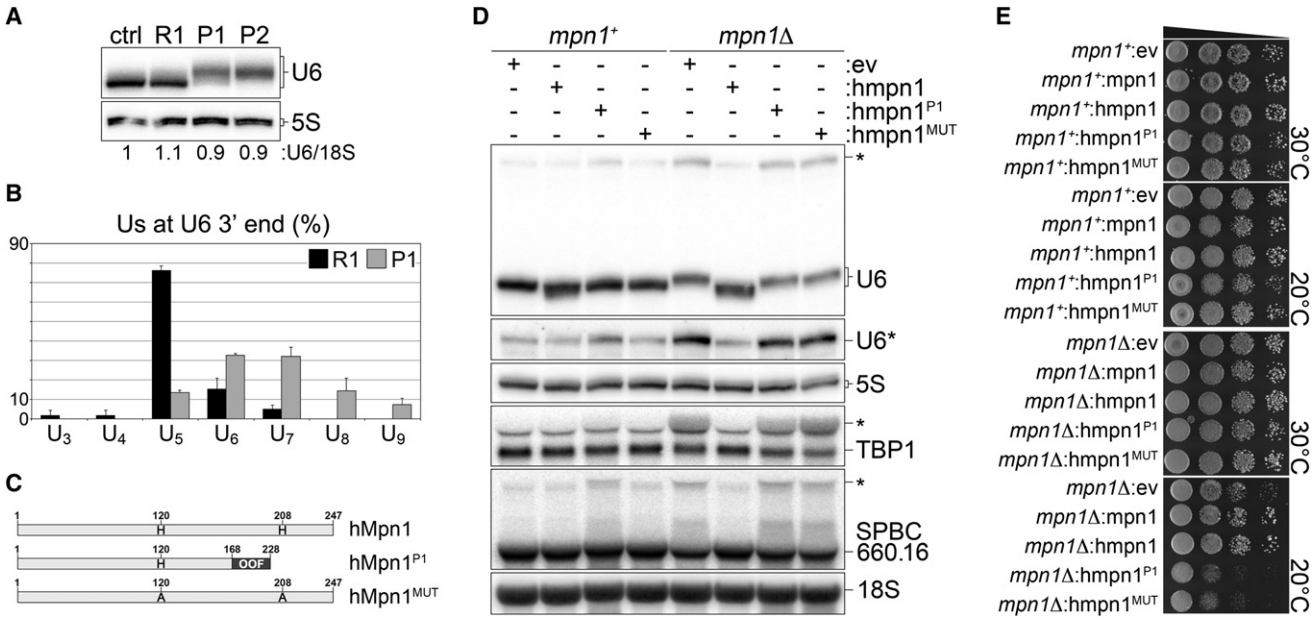

Figure 4. Conservation of Function among Yeast and Human Mpn1 Proteins

(A) Northern blot analysis of U6 in RNA prepared from lymphoblasts established from two independent PN patients (P1 and P2), the healthy brother of P1 (R1), and an unrelated healthy donor (ctrl). Numbers at the bottom are normalized ratios between total U6 and 18S rRNA, as measured by quantitative real-time RT-PCR.

(B) 3′ RACE analysis of U6 oligo(U) tails in R1 and P1 cells. Bars and error bars are averages of the number of Us within U6 oligo(U) tails and SEM from two independent experiments.

(C) Schematic representation of human Mpn1 proteins. In hMpn1^{P1}, protein conservation is lost at position 168 (OOF: out of frame). hMpn1^{MUT} carries histidine-to-alanine substitutions at the indicated positions.

(D) Northern blot analysis of U6 3′ end processing in the indicated yeast strains transformed with plasmids expressing hMpn1 variants. Asterisks indicate intron-containing RNAs.

(E) Replicates of serial dilutions of the indicated yeasts were spotted on complete medium and grown at 20°C or 30°C.

See also Figures S4 and S5.

with *mpn1*$^{+}$ deletion, indicating that pre-mRNA splicing in *mpn1*Δ cells is largely derived from the diminished levels of cellular U6. These observations also further support the notion that the retarded growth of *mpn1*Δ cells is attributable to inefficient splicing.

hMpn1 Is a Functional Ortholog of Mpn1

We prepared total RNA from two unrelated lymphoblastoid cell lines established from two patients affected by PN (hereafter, P1 and P2; Figure 4A) and from two control cell lines established from an unrelated healthy individual (ctrl) and from a healthy brother of P1 (relative 1: R1) (Volpi et al., 2010). Total U6 levels were similar in the four cell lines, whereas the U6 snRNA electrophoretic run was retarded in both P1 and P2 compared to the two control samples (Figure 4A). Most U6 molecules from R1 terminated with an oligo(U) tract comprising five Us and refractory to PAP-mediated nucleotide elongation in the absence of PNK treatment; in contrast, the majority of U6 transcripts in P1 terminated with six to nine Us and were largely elongated by PAP to similar extents in PNK-treated and PNK-untreated samples (Figures 4B and S2C). Thus, hMpn1 deficiency leads to aberrant U6 processing, similar to what was observed in yeast cells. Deep sequencing of the entire poly(A)$^{+}$ transcriptome of R1, P1, and P2 cell lines and RT-PCR analysis of the two randomly chosen *RAD9A* and *CYC1* gene transcripts did not reveal any obvious accumulation of intron-containing pre-mRNAs in PN cells, indicating that these particular cell lines do not suffer from a generalized splicing defect (Figures S5A and S5B).

Next, we generated yeast expression vectors carrying alleles of hMpn1 corresponding to WT hMpn1, to mutant hMpn1 carried by P1 (hMpn1^{P1} in Figure 4C), and to hMpn1 carrying two histidine-to-alanine substitutions in its tetrapeptide motifs (H120 and H208; hMpn1^{MUT} in Figure 4C). The WT hMpn1 completely rescued the defects in U6 processing, pre-mRNA splicing, and growth in the cold when expressed in *mpn1*Δ yeast cells, but it did not affect any of these parameters in WT yeast cells (Figures 4D and 4E). In contrast, hMpn1^{P1} and hMpn1^{MUT} were unable to restore U6 processing in *mpn1*Δ cells and further exacerbated the accumulation of unspliced pre-mRNAs and slow growth in the cold (Figures 4D and 4E). All hMpn1 proteins were expressed at similar levels in all yeast cells whether deficient in Mpn1 or not (Figure S4B).

hMpn1 Physically Interacts with the NTC Complex

We generated different human immortal cell lines stably expressing strep-HA-tagged hMpn1 (hMpn1-SHA). hMpn1-SHA localized predominantly to the nucleus in HeLa cells, as shown by indirect immunofluorescence (Figure S4G), and copurified with U6 snRNA in streptavidin-purification experiments performed

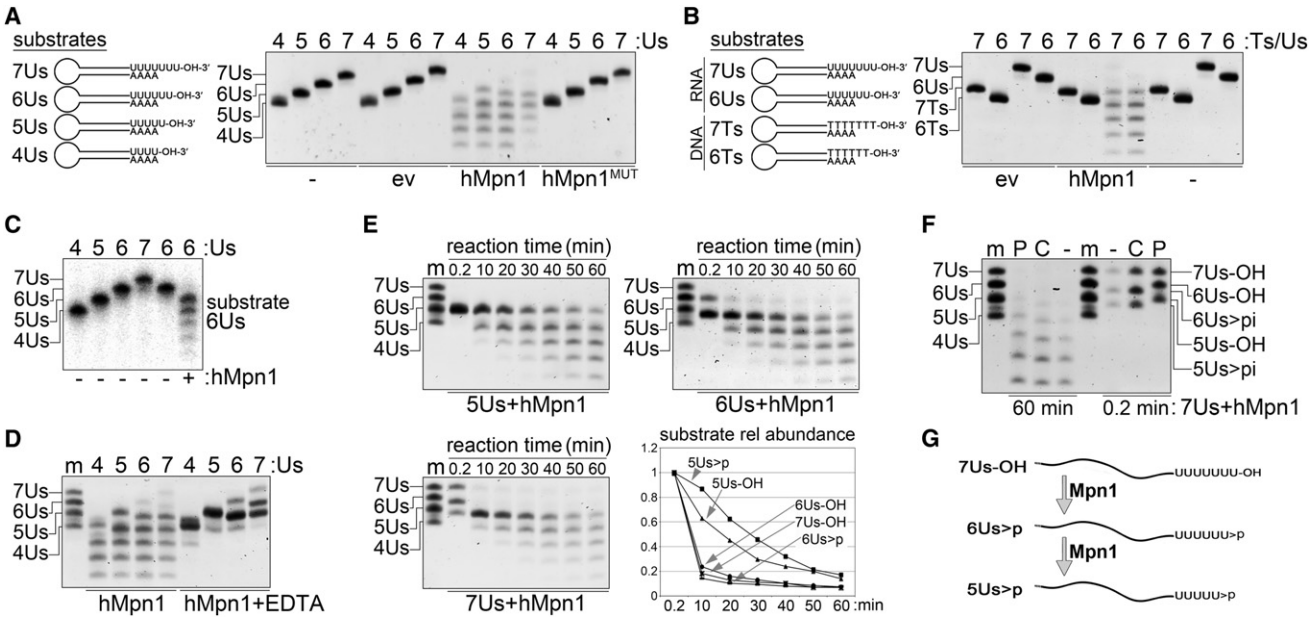

Figure 5. Analysis of hMpn1 Activity In Vitro

(A) Recombinant hMpn1 or hMpn1^{MUT} were incubated with the indicated RNA oligonucleotide substrates, mimicking the structured U6 snRNA 3′ terminus, for 1 hr. As a control, reactions were also performed with buffer only (-) or with empty vector (ev) purifications. RNA products were resolved in denaturing polyacrylamide gels.

(B) hMpn1 was incubated with analogous RNA and DNA substrates for 1 hr.

(C) 6Us RNA substrate was 5′-end radioactively labeled and incubated with hMpn1 for 1 hr. Reaction products were separated as above, and radioactive signal was detected.

(D) The indicated substrates were treated with recombinant hMpn1 in the presence or absence of 20 mM EDTA for 1 hr.

(E) The indicated substrates were incubated with hMpn1, and reaction aliquots were taken at the indicated time points. The graph shows quantifications of the signals at each time point after setting to 1 the value corresponding to the sum of substrates and products measured for the first time point.

(F) 7Us RNA substrate was incubated with hMpn1 for 60 min or 0.2 min, and reaction products were treated with PNK in mild acidic conditions or with CIP prior to gel electrophoresis.

(G) Schematic representation of Mpn1 enzymatic activity in vitro. In all panels, "m" indicates the mix of the four RNA substrates used as a molecular-weight marker.

See also Figure S6.

with the use of hMpn1-SHA-expressing HEK293T cells (Figure S4C). Fractions containing hMpn1-SHA were also strongly enriched in U5 snRNA, but not in U1 and U4 snRNAs or tRNA^{Glu} (Figure S4C). Moreover, mass spectrometric analysis of the same purification samples revealed the presence of PRP19, CDC5L, and PLRG1 polypeptides, which are core components of the human NTC (Figure S4D). The physical interaction between hMpn1-SHA and NTC members was further confirmed with antibodies for human PRP19, CDC5L, and PLRG1 (Figure S4E). These data are consistent with high-throughput interaction experiments indicating that the putative budding yeast and *Drosophila melanogaster* orthologs of Mpn1 (Usb1/YLR132C and CG167090, respectively) physically interact with Prp19 proteins (Giot et al., 2003; Hazbun et al., 2003; Krogan et al., 2006; Yu et al., 2008). Altogether, these results imply that Mpn1 and hMpn1 are functional orthologs promoting U6 processing in distantly related eukaryotes. In addition, the enrichment of U5 snRNA in hMpn1 purification fractions suggests that hMpn1 might be a novel component of the 35S U5 snRNP, which has been shown to contain NTC factors (Makarov et al., 2002; Makarova et al., 2004).

hMpn1 Is a 3′-to-5′ RNA Exonuclease that Processes U6 Oligo(U) Tails In Vitro

To test the putative enzymatic activity of Mpn1 proteins, we purified recombinant, C-terminally histidine-tagged hMpn1 and hMpn1^{MUT} expressed in bacteria (Figure S6A). We incubated the recombinant proteins with RNA oligonucleotides mimicking the structured 3′ end of free human U6 (Rinke et al., 1985), terminating with four to seven Us (substrates: 4Us, 5Us, 6Us, and 7Us, respectively). Due to self-annealing, the four different substrates are expected to generate hairpin structures with stems exposing zero, one, two, or three Us, respectively (Figure 5A). Upon incubation with hMpn1, all substrates were processed into a ladder of shorter species differing from each other by one nucleotide; no oligonucleotide substrate was processed by mock purification extracts or hMpn1^{MUT} (Figure 5A). Thus, hMpn1 shows ribonuclease (RNase) activity that depends on the two histidines within its tetrapeptide motifs. Recombinant hMpn1, but not hMpn1^{MUT}, processed shorter 6Us RNA oligonucleotides that were unable to form secondary structures (linear 6Us: 6Us^{LIN}) mainly into 5Us oligonucleotides (Figure S6B), as observed for structured 6Us. This indicates that the number of Us within the

oligo(U) tract, not its secondary structure, regulates hMpn1 nuclease activity. hMpn1 did not process analogous DNA oligonucleotides terminating with six or seven thymines (substrates: 6Ts and 7Ts, respectively; Figure 5B), revealing hMpn1 specificity for RNA. hMpn1-dependent processing was executed in a 3′-to-5′ direction, as revealed by reactions performed using 6Us oligonucleotides radioactively labeled at their 5′ end (Figure 5C). hMpn1 actively processed RNA substrates in the absence of ATP and metal ions and under different pH conditions (Figure S6C). The addition of EDTA to the reaction did not block hMpn1 activity, although 6Us and 7Us were processed only into 5Us, whereas 5Us and 4Us were very poorly processed (Figures 5D, S6B, and S6C). This suggests that hMpn1 shows a preference for substrates terminating with six or seven Us. Consistently, time-course experiments clearly showed that 6Us and 7Us are quickly trimmed to 5Us within the first few minutes of the reaction (Figures 5E and S6B). Finally, we noticed that hMpn1-processed products ran faster than synthesized oligonucleotides of the same length containing terminal -OH groups, possibly due to the presence of a phosphate group at the 3′ end of hMpn1 products (Figures 5A–5E). Treatment with PNK under mild acidic conditions, but not with CIP, converted hMpn1 products into more slowly migrating forms, indicating that hMpn1 products terminate with a 3′ >p group (Figure 5F). The observations that Mpn1 exonucleolitic activity generates >p groups and is not fully inhibited in the presence of EDTA suggest that Mpn1 could be a metal-ion-independent RNase, although additional experiments are needed to confirm this supposition. Moreover, the presence of a terminal >p group did not affect the ability of hMpn1 to quickly process 6Us >p (produced from processing of 7Us-OH substrates) into 5Us >p, whereas both 5Us >p and 5Us-OH were processed with slow kinetics (Figure 5E). Thus, hMpn1 processes oligo(U) terminating with >p or -OH groups with similar efficiencies. In summary, hMpn1 is a 3′-to-5′ RNA exonuclease that is able to trim U6 oligo(U) tails into shorter tracts terminating with 3′ end >p groups (Figure 5G). This is highly consistent with the U6 snRNA molecular defects in PN cells, wherein we observe accumulation of U6 molecules terminating with 6Us-OH or 7Us-OH, which correspond to efficient substrates for hMpn1 in vitro (Figures 4A and 4B). The ability of hMpn1 to rescue the U6-processing defects of *mpn1*Δ yeasts (Figure 4D) indicates that human and fission yeast Mpn1 proteins share the same catalytic activity.

Mpn1 Sustains U6 Stability

The diminished U6 cellular levels in *mpn1*Δ yeast cells and the altered chemical composition of U6 oligo(U) tracts in Mpn1-deficient yeast and human cells suggest the possibility that the stability of U6 molecules could be altered. We measured the degradation rates of yeast U6 transcripts by inhibiting RNAPIII with the specific inhibitor ML-60218 (Wu et al., 2003) in WT and *mpn1*Δ yeast cells over the course of 12 hr. To monitor the degradation of similar starting amounts of U6 molecules, we also included in the same set of experiments *mpn1*Δ cells carrying one additional copy of the U6 gene (*mpn1*Δ:snU6). In WT cells, U6 levels declined linearly throughout the time period and were reduced to approximately 60% of the starting amount of U6 by the end of the experiment (Figures 6A and 6C). In both *mpn1*$^{+}$-deleted strains, U6 levels dropped precipitously during the first 3 hr to approximately 40% and then slowly decreased further to 30% during the remaining 9 hr (Figures 6A and 6C). The long-lived 5S small RNA was stable during the entire time period, whereas leucine tRNA decayed similarly in both normal and *mpn1*$^{+}$-deficient cells (Figure 6A). In accordance with the increased degradation rates of U6, *mpn1*Δ and *mpn1*Δ:snu6 cells were more sensitive than WT cells when grown in medium containing ML-60218 (data not shown).

An analogous situation was observed in human cells treated with actinomycin D for inhibition of global transcription over 12 hr. U6 transcripts declined with fairly linear kinetics in healthy R1 lymphoblasts and had a calculated half-life of approximately 4.7 hr (Figures 6B and 6C). In PN-affected P1 and P2 cells, U6 decay was faster, especially during the first 3 hr of treatment. The U6 half-life was approximately 1.7 hr in P1 cells and 2.8 hr in P2 cells (Figures 6B and 6C). As for yeast cells, 5S RNA steady-state levels remained constant during the time course in the three cell lines (Figure 6B). Altogether, these observations indicate that U6 transcripts are less stable in Mpn1-deficient yeast and human cells and suggest that Mpn1-mediated processing of U6 oligo(U) tails prevents U6 snRNA degradation.

DISCUSSION

We have demonstrated here that U6 molecules that fail to be posttranscriptionally modified by Mpn1 are rapidly directed toward degradation, thereby establishing Mpn1 as a regulator of U6 stability (Figure 6D). Similar conclusions have been recently reached for Usb1p, the *Saccharomyces cerevisiae* ortholog of Mpn1, further supporting the evolutionary conservation of Mpn1-associated functions (Mroczek et al., 2012). Extending beyond this notion, we have also shown that Mpn1 is an actual RNA exonuclease and that the stability of U6 molecules is compromised in lymphoblastoid cells established from patients affected by PN. It is now necessary to understand the details of the molecular mechanisms through which Mpn1 antagonizes U6 degradation. In vitro experiments have clearly shown that the presence of a terminal >p group on U6 enhances its affinity for the LSm2–8 complex and inversely reduces La protein binding (Licht et al., 2008). Therefore, it is conceivable that binding of the LSm2–8 complex stabilizes U6 by hiding its 3′ end from degradation machineries. Still, a more direct function could also be envisaged for the >p group. A fraction of *Drosophila melanogaster* and budding yeast U6 snRNA was reported to be 3′ polyadenylated by the noncanonical PAP Trf4, and thus directed toward degradation through the nuclear exosome (Nakamura et al., 2008; Wyers et al., 2005). A similar mechanism might also exist in humans, given that a small fraction of U6 molecules from HeLa cells contain a posttranscriptionally added adenylic acid residue at their 3′ ends (Chen et al., 2000; Sinha et al., 1998). Because Trf4 requires a free 3′-OH terminal group for it to be able to add nucleotides, the presence of a terminal >p group on U6 is expected to physically hinder Trf4-mediated polyadenylation. Regardless of the actual molecular mechanism through which Mpn1 protects U6 from degradation, our results suggest the existence of a thus far unappreciated quality-control pathway, perhaps coupled with pre-mRNA

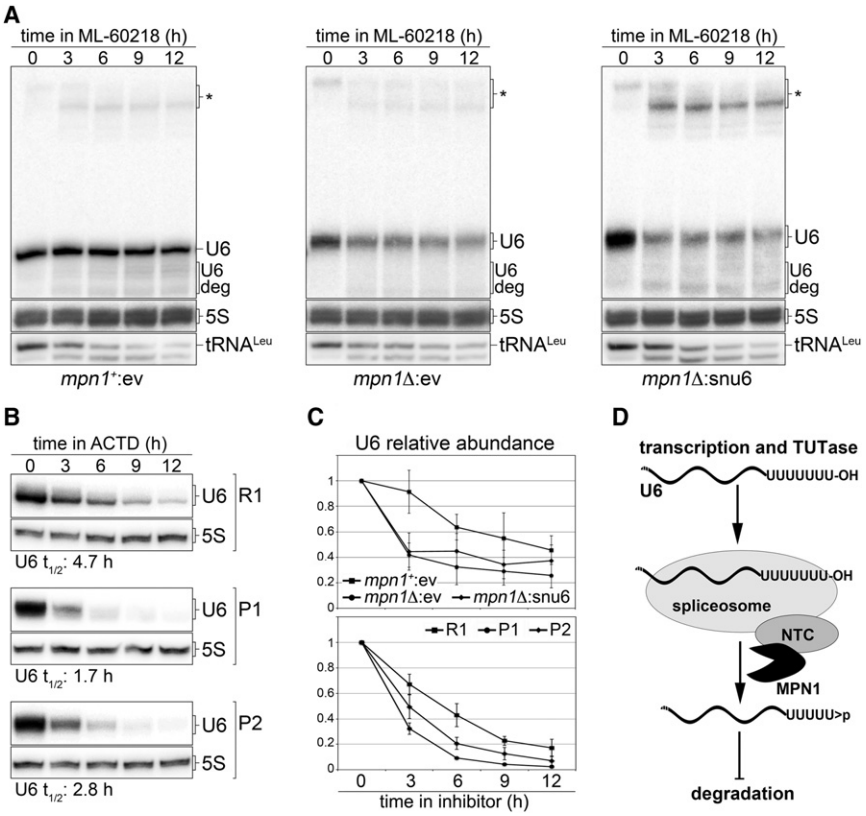

Figure 6. Reduced Stability of U6 snRNA in Human and Yeast Mpn1-Deficient Cells

(A) The indicated yeast cells were treated with ML-60218 for a total of 12 hr, and RNA samples were prepared every 3 hr. RNA was subjected to northern blot analysis. Asterisks indicate premature U6 and putative products generated by RNAPIII premature termination. U6 deg, putative degradation products of U6; $tRNA^{Leu}$, leucine tRNA.

(B) R1, P1, and P2 lymphoblasts were treated with actinomycin D (ACTD) for 12 hr. RNA samples were prepared every 3 hr and processed via northern blotting for detection of U6 and 5S RNAs. Calculated half-lives ($t_{1/2}$) of U6 are indicated for the different cell lines.

(C) Quantification of U6 RNA levels in yeast (upper graph) and human (lower graph) cells upon transcription inhibition. For each sample, U6 signals were normalized through the corresponding 5S signals and successively expressed as fold decrease over U6 signal at time 0. Values and error bars are means and SEM from three to five independent experiments.

(D) Model depicting Mpn1-associated functions in U6 processing and stabilization. See Discussion for details.

splicing, that may decide whether or not specific U6 molecules need to be eliminated from the cell (Figure 6D).

By showing that Mpn1 is the 3′-to-5′ exonuclease that trims U6 3′ end oligo(U) tails, we have also revealed the identity of the enzyme that counteracts TUTase in vivo. Our data indicate that Mpn1 alone is sufficient not only to restrict U6 oligo(U) tails but also to introduce the >p group found on the large majority of cellular U6 (Figure 6D). The point at which Mpn1 accesses and modifies U6 remains to be determined. However, the evolutionarily conserved physical interaction of Mpn1 with the spliceosome-associated NTC complex suggests that Mpn1 could modify U6 within the active spliceosome upon NTC-mediated recruitment to the 35S U5 snRNP (Makarov et al., 2002; Makarova et al., 2004) (Figure 6D). This idea is consistent with experiments performed with the use of HeLa nuclear extracts showing that long U6 molecules terminating with -OH groups can enter the spliceosome and that some of these shorten with time as splicing proceeds (Tazi et al., 1993).

It has been proved that diminished expression or deletion of several yeast NTC proteins results in reduced recycling of U6 molecules upon splicing completion and consequent accumulation of free U4 (Chen et al., 2006; Lygerou et al., 1999). Although the lower levels of cellular U6 present in *mpn1*Δ cells are per se sufficient to explain the diminished levels of U4/U6 di-snRNPs and the inefficient pre-mRNA splicing, the observations just mentioned suggest that U6 recycling might also be impaired in Mpn1-deficient cells and that the recycling defects observed in NTC mutants might stem, at least in part, from a lack of Mpn1-mediated processing of U6. Intriguingly, the LSm2–8 ring promotes U6 recycling through the recruitment of the U4/U6 annealing factor Prp24/p110 (Bell et al., 2002; Martin-Tumasz et al., 2011; Pannone et al., 1998; Raghunathan and Guthrie, 1998; Ryan et al., 2002). These observations, together with the already-mentioned notion that a terminal >p group on U6 augments its affinity for the LSm2–8 complex (Licht et al., 2008), make it tempting to speculate that Mpn1 enzymatic activity could promote U6 recycling by allowing LSm2–8 and Prp24/p100 binding to U6.

Our work also provides a framework in which to better understand the pathogenesis of PN. Although the accumulation of intron-containing pre-mRNA molecules in *mpn1*Δ yeasts suggests that inefficient splicing could be the molecular trigger of PN, the lack of a generalized splicing defect observed in PN lymphoblasts seems to contradict this hypothesis. Still, it is possible that Mpn1 deficiency can be better tolerated in human cells than in yeasts due to higher U6 cellular levels. Indeed, the human genome possesses at least five transcriptionally active U6 snRNA genes (Domitrovich and Kunkel, 2003), and we have clearly shown that insertion of one extra copy of the U6 gene in *mpn1*Δ cells is sufficient to avert splicing defects. Hence, pre-mRNA splicing could be affected only in cell types wherein U6 cellular levels are limiting. For example, U6 transcripts are downregulated in rat bone marrow cells during development (Ray et al., 1997). Similarly, exogenous insults such as UV light irradiation are known to reduce U6 steady-state levels (Choudhury et al., 1988); interestingly, in this regard, some PN patients have been diagnosed with light sensitivity of the skin (Arnold et al., 2010). Therefore, Mpn1 deficiency might have a different

impact on the cell according to the tissue- and developmental-stage-specific expression of U6 snRNA, as well as the environmental conditions. This hypothesis could explain why only a limited number of tissues are affected in PN patients (Colombo et al., 2012). An alternative but not mutually exclusive hypothesis is that Mpn1 might modify RNA substrates other than U6 snRNA to possibly regulate their stability. Compromised metabolism of these yet-to-be-discovered RNAs might be responsible for PN pathogenesis. As with our PN cells, mouse embryonic fibroblasts knocked out for the NTC member PLRG1 also failed to show a generalized splicing defect (Kleinridders et al., 2009). Moreover, members of the mammalian NTC complex have been implicated in several nonsplicing mechanisms, including cellular senescence, the DNA damage response, and interstrand crosslink repair (Legerski, 2009). Mpn1 and other members of the NTC complex could cooperatively regulate the stability of ncRNA species involved in these different cellular pathways, thus explaining the pleiotropism of PN.

EXPERIMENTAL PROCEDURES

Yeast Strains

Original *Schizosaccharomyces pombe* strains were kind gifts of J. P. Cooper and R. Allshire or were purchased from Bioneer (see Table S1). Where indicated, yeast strains were transformed with pCST159-derived plasmids in order to obtain stable integrants upon Aureobasidin selection.

Human Cell Lines

Lymphoblastoid cell lines were obtained from Lidia Larizza (University of Milano, Italy), Galliera Genetic Bank (Genova, Italy), and Alessandra Renieri (University of Siena, Italy). ML07136M (P1 in the text) and RT1 (P2) are SV40-immortalized lymphoblastoid cell lines derived from two independent PN patients, and GGB04410M (R1) is derived from a healthy brother of P1 (Volpi et al., 2010). MR140 (ctrl) is an SV40-immortalized lymphoblastoid cell line derived from a completely unrelated healthy individual. To generate stable cell lines expressing hMpn1, we transduced HEK293T and HeLa cells with retroviruses expressing strep-HA-tagged hMpn1 (pBABE-Hygro-hMpn1) or with empty vector control retroviruses.

RNA Extraction and Analysis

Total yeast RNA was extracted with the use of hot phenol according to standard procedures. Total human RNA was prepared with TRIzol (Invitrogen) followed by column purification with the Direct-zol kit (Zymo Research). RNA was subjected to DNase I digestion at least once before further procedures. To remove 3′ terminal phosphate groups from RNA, we used T4 PNK (New England BioLabs [NEB]) following published protocols (Schürer et al., 2002). CIP (NEB) treatment was performed according to the manufacturer's instructions. For native PAGE, RNA was extracted with cold phenol and resolved in a 5% nondenaturing polyacrylamide-Tris-borate-EDTA gel. For 3′ RACE experiments, we used PNK- and PAP-treated total RNA and the FirstChoice RLM-RACE kit (Ambion) according to the manufacturer's instructions. RNA-seq was performed on poly(A)$^+$ RNA purified with the TrueSeq SBS RNA kit v5 (Illumina) with the use of the Illumina HiSeq 2000 platform at FASTERIS (Plan-les-Ouates, Switzerland).

Mpn1 Nuclease Assay

Recombinant hMpn1 proteins were purified with the HisPur Cobalt Resin (Thermo Scientific) according to the manufacturer's instructions. RNA and DNA oligonucleotide substrates were synthesized and gel-purified at Microsynth AG (Balgach, Switzerland). Oligonucleotide substrates (see Table S2) were mixed in 20 mM Tris-HCl (pH 7.4), 100 mM NaCl, and 0.005% Tween 20. The mixture was incubated at 65°C for 5 min, cooled down to 37°C at a rate of 0.05°C/s, and quickly passed to ice. After the addition of 1 μl of recombinant hMpn1 (36 pmol/μl), reactions were incubated for the indicated time at 37°C. Reactions were stopped via the addition of equal volumes of electrophoresis loading buffer containing 8 M urea and incubation at 90°C for 5 min. Samples were loaded directly in denaturing polyacrylamide gels.

ACCESSION NUMBERS

Raw sequencing data for the transcriptome of lymphoblastoid cell lines have been deposited in the ArrayExpress database under accession number E-MTAB-1197 (http://www.ebi.ac.uk/arrayexpress/).

SUPPLEMENTAL INFORMATION

Supplemental Information includes Extended Experimental Procedures, six figures, and three tables and can be found with this article online at http://dx.doi.org/10.1016/j.celrep.2012.08.031.

LICENSING INFORMATION

ACKNOWLEDGMENTS

We thank Amadou Bah and Luca Lorenzi for help during the initial development of this project; Julie P. Cooper and Robin Allshire for yeast strains; Lidia Larizza, Alessandra Renieri, and Galliera Genetic Bank for lymphoblastoid cells; Vikram Panse and Matthias Gstaiger for reagents; and Olga Murina and the Azzalin laboratory for helpful discussions. We also thank Mauro Delorenzi from the Bioinformatics Core Facility of the SIB Swiss Institute of Bioinformatics for discussions and critical reading of the manuscript. This work was supported by the European Research Council (BFTERRA to C.M.A.), the Swiss National Science Foundation (PP00P3-123356 to C.M.A.), Fondazione Cariplo (2008-2507 to C.M.A.), and the SIB Swiss Institute of Bioinformatics (biostatistical services of the Bioinformatics Core Facility). V.S., H.W., and C.M.A. performed the experiments and analyzed the data. E.M. and C.S. analyzed the RNA deep-sequencing data. V.S. and C.M.A. wrote the manuscript.

Received: July 25, 2012
Revised: August 31, 2012
Accepted: August 31, 2012
Published online: September 27, 2012

REFERENCES

Achsel, T., Brahms, H., Kastner, B., Bachi, A., Wilm, M., and Lührmann, R. (1999). A doughnut-shaped heteromer of human Sm-like proteins binds to the 3′-end of U6 snRNA, thereby facilitating U4/U6 duplex formation in vitro. EMBO J. *18*, 5789–5802.

Arnold, A.W., Itin, P.H., Pigors, M., Kohlhase, J., Bruckner-Tuderman, L., and Has, C. (2010). Poikiloderma with neutropenia: a novel C16orf57 mutation and clinical diagnostic criteria. Br. J. Dermatol. *163*, 866–869.

Azzalin, C.M., Reichenbach, P., Khoriauli, L., Giulotto, E., and Lingner, J. (2007). Telomeric repeat containing RNA and RNA surveillance factors at mammalian chromosome ends. Science *318*, 798–801.

Bah, A., Wischnewski, H., Shchepachev, V., and Azzalin, C.M. (2012). The telomeric transcriptome of Schizosaccharomyces pombe. Nucleic Acids Res. *40*, 2995–3005.

Bell, M., Schreiner, S., Damianov, A., Reddy, R., and Bindereif, A. (2002). p110, a novel human U6 snRNP protein and U4/U6 snRNP recycling factor. EMBO J. *21*, 2724–2735.

Box, J.A., Bunch, J.T., Tang, W., and Baumann, P. (2008). Spliceosomal cleavage generates the 3′ end of telomerase RNA. Nature *456*, 910–914.

Chantorn, R., and Shwayder, T. (2012). Poikiloderma with neutropenia: report of three cases including one with calcinosis cutis. Pediatr. Dermatol. *29*, 463–472.

Chen, Y., Sinha, K., Perumal, K., and Reddy, R. (2000). Effect of 3′ terminal adenylic acid residue on the uridylation of human small RNAs in vitro and in frog oocytes. RNA *6*, 1277–1288.

Chen, C.H., Kao, D.I., Chan, S.P., Kao, T.C., Lin, J.Y., and Cheng, S.C. (2006). Functional links between the Prp19-associated complex, U4/U6 biogenesis, and spliceosome recycling. RNA *12*, 765–774.

Choudhury, K., Choudhury, I., Jones, R.W., Thirunavukkarasu, C., and Eliceiri, G.L. (1988). Metabolism of U6 RNA species in nonirradiated and UV-irradiated mammalian cells. J. Cell. Physiol. *137*, 529–536.

Clericuzio, C., Hoyme, H.E., and Asse, J.M. (1991). Immune deficient poikiloderma: A new genodermatosis. Am. J. Hum. Genet. Suppl. *49*, A661.

Clericuzio, C., Harutyunyan, K., Jin, W., Erickson, R.P., Irvine, A.D., McLean, W.H., Wen, Y., Bagatell, R., Griffin, T.A., Shwayder, T.A., et al. (2011). Identification of a novel C16orf57 mutation in Athabaskan patients with Poikiloderma with Neutropenia. Am. J. Med. Genet. A. *155A*, 337–342.

Colombo, E.A., Bazan, J.F., Negri, G., Gervasini, C., Elcioglu, N.H., Yucelten, D., Altunay, I., Cetincelik, U., Teti, A., Del Fattore, A., et al. (2012). Novel C16orf57 mutations in patients with Poikiloderma with Neutropenia: bioinformatic analysis of the protein and predicted effects of all reported mutations. Orphanet J. Rare Dis. *7*, 7.

Concolino, D., Roversi, G., Muzzi, G.L., Sestito, S., Colombo, E.A., Volpi, L., Larizza, L., and Strisciuglio, P. (2010). Clericuzio-type poikiloderma with neutropenia syndrome in three sibs with mutations in the C16orf57 gene: delineation of the phenotype. Am. J. Med. Genet. A. *152A*, 2588–2594.

Domitrovich, A.M., and Kunkel, G.R. (2003). Multiple, dispersed human U6 small nuclear RNA genes with varied transcriptional efficiencies. Nucleic Acids Res. *31*, 2344–2352.

Giot, L., Bader, J.S., Brouwer, C., Chaudhuri, A., Kuang, B., Li, Y., Hao, Y.L., Ooi, C.E., Godwin, B., Vitols, E., et al. (2003). A protein interaction map of Drosophila melanogaster. Science *302*, 1727–1736.

Gu, J., Shumyatsky, G., Makan, N., and Reddy, R. (1997). Formation of 2′,3′-cyclic phosphates at the 3′ end of human U6 small nuclear RNA in vitro. Identification of 2′,3′-cyclic phosphates at the 3′ ends of human signal recognition particle and mitochondrial RNA processing RNAs. J. Biol. Chem. *272*, 21989–21993.

Hazbun, T.R., Malmström, L., Anderson, S., Graczyk, B.J., Fox, B., Riffle, M., Sundin, B.A., Aranda, J.D., McDonald, W.H., Chiu, C.H., et al. (2003). Assigning function to yeast proteins by integration of technologies. Mol. Cell *12*, 1353–1365.

Kleinridders, A., Pogoda, H.M., Irlenbusch, S., Smyth, N., Koncz, C., Hammerschmidt, M., and Brüning, J.C. (2009). PLRG1 is an essential regulator of cell proliferation and apoptosis during vertebrate development and tissue homeostasis. Mol. Cell. Biol. *29*, 3173–3185.

Krogan, N.J., Cagney, G., Yu, H., Zhong, G., Guo, X., Ignatchenko, A., Li, J., Pu, S., Datta, N., Tikuisis, A.P., et al. (2006). Global landscape of protein complexes in the yeast Saccharomyces cerevisiae. Nature *440*, 637–643.

Kunkel, G.R., Maser, R.L., Calvet, J.P., and Pederson, T. (1986). U6 small nuclear RNA is transcribed by RNA polymerase III. Proc. Natl. Acad. Sci. USA *83*, 8575–8579.

Legerski, R.J. (2009). The Pso4 complex splices into the DNA damage response. Cell Cycle *8*, 3448–3449.

Licht, K., Medenbach, J., Lührmann, R., Kambach, C., and Bindereif, A. (2008). 3′-cyclic phosphorylation of U6 snRNA leads to recruitment of recycling factor p110 through LSm proteins. RNA *14*, 1532–1538.

Lund, E., and Dahlberg, J.E. (1992). Cyclic 2′,3′-phosphates and nontemplated nucleotides at the 3′ end of spliceosomal U6 small nuclear RNA's. Science *255*, 327–330.

Lygerou, Z., Christophides, G., and Séraphin, B. (1999). A novel genetic screen for snRNP assembly factors in yeast identifies a conserved protein, Sad1p, also required for pre-mRNA splicing. Mol. Cell. Biol. *19*, 2008–2020.

Makarov, E.M., Makarova, O.V., Urlaub, H., Gentzel, M., Will, C.L., Wilm, M., and Lührmann, R. (2002). Small nuclear ribonucleoprotein remodeling during catalytic activation of the spliceosome. Science *298*, 2205–2208.

Makarova, O.V., Makarov, E.M., Urlaub, H., Will, C.L., Gentzel, M., Wilm, M., and Lührmann, R. (2004). A subset of human 35S U5 proteins, including Prp19, function prior to catalytic step 1 of splicing. EMBO J. *23*, 2381–2391.

Martin-Tumasz, S., Richie, A.C., Clos, L.J., 2nd, Brow, D.A., and Butcher, S.E. (2011). A novel occluded RNA recognition motif in Prp24 unwinds the U6 RNA internal stem loop. Nucleic Acids Res. *39*, 7837–7847.

Mayes, A.E., Verdone, L., Legrain, P., and Beggs, J.D. (1999). Characterization of Sm-like proteins in yeast and their association with U6 snRNA. EMBO J. *18*, 4321–4331.

Mazumder, R., Iyer, L.M., Vasudevan, S., and Aravind, L. (2002). Detection of novel members, structure-function analysis and evolutionary classification of the 2H phosphoesterase superfamily. Nucleic Acids Res. *30*, 5229–5243.

Mroczek, S., Krwawicz, J., Kutner, J., Lazniewski, M., Kucinski, I., Ginalski, K., and Dziembowski, A. (2012). C16orf57, a gene mutated in poikiloderma with neutropenia, encodes a putative phosphodiesterase responsible for the U6 snRNA 3′ end modification. Genes Dev. *26*, 1911–1925.

Nakamura, R., Takeuchi, R., Takata, K., Shimanouchi, K., Abe, Y., Kanai, Y., Ruike, T., Ihara, A., and Sakaguchi, K. (2008). TRF4 is involved in polyadenylation of snRNAs in Drosophila melanogaster. Mol. Cell. Biol. *28*, 6620–6631.

Pannone, B.K., Xue, D., and Wolin, S.L. (1998). A role for the yeast La protein in U6 snRNP assembly: evidence that the La protein is a molecular chaperone for RNA polymerase III transcripts. EMBO J. *17*, 7442–7453.

Piard, J., Holder-Espinasse, M., Aral, B., Gigot, N., Rio, M., Tardieu, M., Puzenat, E., Goldenberg, A., Toutain, A., Franques, J., et al. (2012). Systematic search for neutropenia should be part of the first screening in patients with poikiloderma. Eur. J. Med. Genet. *55*, 8–11.

Potashkin, J., Li, R., and Frendewey, D. (1989). Pre-mRNA splicing mutants of Schizosaccharomyces pombe. EMBO J. *8*, 551–559.

Raghunathan, P.L., and Guthrie, C. (1998). A spliceosomal recycling factor that reanneals U4 and U6 small nuclear ribonucleoprotein particles. Science *279*, 857–860.

Ray, R., Ray, K., and Panda, C.K. (1997). Differential alterations in metabolic pattern of the six major UsnRNAs during development. Mol. Cell. Biochem. *177*, 79–88.

Rinke, J., and Steitz, J.A. (1985). Association of the lupus antigen La with a subset of U6 snRNA molecules. Nucleic Acids Res. *13*, 2617–2629.

Rinke, J., Appel, B., Digweed, M., and Lührmann, R. (1985). Localization of a base-paired interaction between small nuclear RNAs U4 and U6 in intact U4/U6 ribonucleoprotein particles by psoralen cross-linking. J. Mol. Biol. *185*, 721–731.

Ryan, D.E., Stevens, S.W., and Abelson, J. (2002). The 5′ and 3′ domains of yeast U6 snRNA: Lsm proteins facilitate binding of Prp24 protein to the U6 telestem region. RNA *8*, 1011–1033.

Salgado-Garrido, J., Bragado-Nilsson, E., Kandels-Lewis, S., and Séraphin, B. (1999). Sm and Sm-like proteins assemble in two related complexes of deep evolutionary origin. EMBO J. *18*, 3451–3462.

Schürer, H., Lang, K., Schuster, J., and Mörl, M. (2002). A universal method to produce in vitro transcripts with homogeneous 3′ ends. Nucleic Acids Res. *30*, e56.

Séraphin, B. (1995). Sm and Sm-like proteins belong to a large family: identification of proteins of the U6 as well as the U1, U2, U4 and U5 snRNPs. EMBO J. *14*, 2089–2098.

Sinha, K.M., Gu, J., Chen, Y., and Reddy, R. (1998). Adenylation of small RNAs in human cells. Development of a cell-free system for accurate adenylation on the 3′-end of human signal recognition particle RNA. J. Biol. Chem. *273*, 6853–6859.

Stefano, J.E. (1984). Purified lupus antigen La recognizes an oligouridylate stretch common to the 3′ termini of RNA polymerase III transcripts. Cell *36*, 145–154.

Tanaka, A., Morice-Picard, F., Lacombe, D., Nagy, N., Hide, M., Taïeb, A., and McGrath, J. (2010). Identification of a homozygous deletion mutation in C16orf57 in a family with Clericuzio-type poikiloderma with neutropenia. Am. J. Med. Genet. A. *152A*, 1347–1348.

Tani, T., and Ohshima, Y. (1989). The gene for the U6 small nuclear RNA in fission yeast has an intron. Nature *337*, 87–90.

Tazi, J., Forne, T., Jeanteur, P., Cathala, G., and Brunel, C. (1993). Mammalian U6 small nuclear RNA undergoes 3′ end modifications within the spliceosome. Mol. Cell. Biol. *13*, 1641–1650.

Terns, M.P., Lund, E., and Dahlberg, J.E. (1992). 3′-end-dependent formation of U6 small nuclear ribonucleoprotein particles in Xenopus laevis oocyte nuclei. Mol. Cell. Biol. *12*, 3032–3040.

Trippe, R., Richly, H., and Benecke, B.J. (2003). Biochemical characterization of a U6 small nuclear RNA-specific terminal uridylyltransferase. Eur. J. Biochem. *270*, 971–980.

Trippe, R., Guschina, E., Hossbach, M., Urlaub, H., Lührmann, R., and Benecke, B.J. (2006). Identification, cloning, and functional analysis of the human U6 snRNA-specific terminal uridylyl transferase. RNA *12*, 1494–1504.

Valadkhan, S. (2010). Role of the snRNAs in spliceosomal active site. RNA Biol. *7*, 345–353.

Vidal, V.P., Verdone, L., Mayes, A.E., and Beggs, J.D. (1999). Characterization of U6 snRNA-protein interactions. RNA *5*, 1470–1481.

Volpi, L., Roversi, G., Colombo, E.A., Leijsten, N., Concolino, D., Calabria, A., Mencarelli, M.A., Fimiani, M., Macciardi, F., Pfundt, R., et al. (2010). Targeted next-generation sequencing appoints c16orf57 as clericuzio-type poikiloderma with neutropenia gene. Am. J. Hum. Genet. *86*, 72–76.

Wahl, M.C., Will, C.L., and Lührmann, R. (2009). The spliceosome: design principles of a dynamic RNP machine. Cell *136*, 701–718.

Walne, A.J., Vulliamy, T., Beswick, R., Kirwan, M., and Dokal, I. (2010). Mutations in C16orf57 and normal-length telomeres unify a subset of patients with dyskeratosis congenita, poikiloderma with neutropenia and Rothmund-Thomson syndrome. Hum. Mol. Genet. *19*, 4453–4461.

Will, C.L., and Lührmann, R. (2011). Spliceosome structure and function. Cold Spring Harb. Perspect. Biol. *3*, a003707. http://dx.doi.org/10.1101/cshperspect.a003707.

Wu, L., Pan, J., Thoroddsen, V., Wysong, D.R., Blackman, R.K., Bulawa, C.E., Gould, A.E., Ocain, T.D., Dick, L.R., Errada, P., et al. (2003). Novel small-molecule inhibitors of RNA polymerase III. Eukaryot. Cell *2*, 256–264.

Wyers, F., Rougemaille, M., Badis, G., Rousselle, J.C., Dufour, M.E., Boulay, J., Régnault, B., Devaux, F., Namane, A., Séraphin, B., et al. (2005). Cryptic pol II transcripts are degraded by a nuclear quality control pathway involving a new poly(A) polymerase. Cell *121*, 725–737.

Yu, H., Braun, P., Yildirim, M.A., Lemmens, I., Venkatesan, K., Sahalie, J., Hirozane-Kishikawa, T., Gebreab, F., Li, N., Simonis, N., et al. (2008). High-quality binary protein interaction map of the yeast interactome network. Science *322*, 104–110.